

Quark model of pion photoproduction from protons by polarized photons in the resonance region*

Steven B. Berger and Bernard T. Feld[†]

Laboratory for Nuclear Science and Department of Physics, Massachusetts Institute of Technology, Cambridge, Massachusetts 02139

(Received 21 April 1975)

Measurements on the photoproduction of pions from protons by polarized photons are compared with predictions of the conventional quark model in the photon energy range 0.8–1.6 GeV. The experimental data, from an MIT-SLAC collaboration, are for the 90° (in the center-of-mass system) production cross section of positive and neutral pions, both along and normal to the direction of polarization of the incident photons. The computations include *s*-channel excitation of all observed resonances of mass up to 2 GeV, but neglect nonresonant background effects. Resonances are assigned to the 56-plet (even parity) and 70-plet (odd parity) representations of $SU(6) \times O(3)$, assuming all baryonic states to be appropriate combinations of three quarks, interacting in an harmonic-oscillator potential. Good qualitative agreement is achieved by appropriate choice of the parameter corresponding to the strength of the potential. A greatly improved fit results from the assignment of the $S_{11}(1535)$ level to the spin-3/2 octet of the 70-plet, first excited baryon supermultiplet. However, attempts at mixing between corresponding levels of the spin-1/2 and spin-3/2 states of this supermultiplet fail to improve the fit. We interpret this as indicating appreciable mixing of the levels concerned with corresponding states of higher supermultiplets of $SU(6)$.

I. INTRODUCTION

Quark models have been applied successfully as a basis for understanding the observed electromagnetic properties of mesonic¹ and baryonic states.² The original and most straightforward quark model³ assumes that hadrons are made up of structureless spin- $\frac{1}{2}$ quarks of three types, $q \equiv \rho, \pi, \lambda$, each carrying baryon number $B = \frac{1}{3}$ and with the other intrinsic quantum numbers, corresponding to isospin (I, I_3), strangeness (S), hypercharge ($Y = B + S$), and electric charge ($e_q/e = I_3 + \frac{1}{2}Y$), as given in Table I.

According to this model, mesonic states are constructed out of quark-antiquark⁴ pairs ($q\bar{q}$) while baryonic states contain a triplet of quarks (qqq). Since the three quarks may be regarded as corresponding to the elements of a fundamental representation of the $SU(3) \times SU(2) = SU(6)$ group, the internal symmetries of the various ($q\bar{q}$) or (qqq) states are respectively derivable from the symmetries of the $6 \times \bar{6}$ or $6 \times 6 \times 6$ representations of this group. Consideration of the spatial symmetries (orbital angular momenta) of the multi-quark systems thus permits classification of all the hadronic states according to the representations of $SU(6) \times O(3)$ or, if the decomposition into intrinsic and spin properties is useful, $SU(3) \times SU(2) \times O(3)$.

The quark combinations appropriate to the various states, available according to this symmetry scheme, and the resulting hadron properties have been considered by, among others, Dalitz,⁵ Faiman and Hendry,⁶ Copley, Karl, and Obryk,⁷ Feshbach and Kisslinger,⁸ Feynman, Kislinger, and

Ravndal,⁹ and Feld.² These investigators have treated the quarks as moving in an effective central field, usually of the harmonic-oscillator variety, generally imposing the requirement that the wave function be symmetrical with respect to interchange of any two quarks. (See, however, Drell and Johnson¹⁰ for a variant that permits the quarks to obey Fermi-Dirac statistics.)

In considering electromagnetic transitions between hadronic states, photon absorption or emission processes are generally computed as a sum of possible transitions involving one quark at a time, using an appropriate approximation of the electromagnetic currents. Most calculations have been based on the assumption of a conventional, nonrelativistic form of the electromagnetic interaction Hamiltonian; however, the results do not appear to be highly sensitive to the treatment in this regard.⁹

The computations of partial widths for photon emission, made on this basis, are in reasonable qualitative agreement with observation,⁶ as are the predicted cross sections for pion photoproduction,⁷ although the latter suffer from ambiguities of interpretation arising from problems of taking proper account of background effects due to other mechanisms (e.g., one-pion and vector-meson exchange,¹¹ or the so-called Born terms¹²).

Photomeson production experiments provide a particularly sensitive test of models of hadronic structure (such as the one here under consideration) since the predictions depend in detail both on the spatial distributions of the hadronic components and on the assumed electromagnetic properties of these components. Observations of angular

TABLE I. Quark properties.

q	B	I	I_3	Y	S	e_q/e
\mathcal{P}	$\frac{1}{3}$	$\frac{1}{2}$	$\frac{1}{2}$	$\frac{1}{3}$	0	$\frac{2}{3}$
\mathcal{N}	$\frac{1}{3}$	$\frac{1}{2}$	$-\frac{1}{2}$	$\frac{1}{3}$	0	$-\frac{1}{3}$
λ	$\frac{1}{3}$	0	0	$-\frac{2}{3}$	-1	$-\frac{1}{3}$

distributions of pions emitted in the absorption of photons of different polarization are especially useful for distinguishing between different models, since such observations could permit the separation of electric and magnetic amplitudes corresponding to specific changes of orbital and spin angular momentum between the ground nucleon state and the excited state to which the hadron is raised by the photon absorption.

In this regard, the photon energy range of $\approx 0.5-1.5$ GeV is the most interesting, since it is above the region of complete dominance of the lowest ($I=J=\frac{3}{2}$) isobar, but still in the resonance energy range (i.e., where resonance spacings are greater than resonance widths), and yet remains below the energy range where the aforementioned background processes dominate over the s -channel resonant photon absorption.

As long as it remains possible to ascribe the meson production at a given energy mainly to the effects of resonant absorption into a single intermediate state, there is a strong correlation between the direction of meson emission and the direction of the photon polarization; this correlation is such that processes dominated by electric multipole absorption and those dominated by magnetic tend to be orthogonal to each other. That is, electric absorption leads to meson production mainly in the plane of polarization (plane of the electric vector), whereas magnetic absorption

gives rise to a tendency for meson emission normal to the polarization direction. Since electric absorption would tend to be enhanced in processes involving simple internal orbital angular momentum changes, while magnetic absorption would be preferred for spin-flip processes, it is not surprising that the computed photoproduction amplitudes will be sensitive to the details of the model of hadronic structure (and the properties of its constituents) being used.¹³

The extent of such correlations may be observed in Table II, in which we have separated the amplitudes for photomeson production into their magnetic and electric components, for absorption into states of angular momentum $\frac{1}{2}-\frac{5}{2}$ and both parities. The photons are assumed incident along the z axis and the mesons emitted along the x axis. The parallel amplitudes (columns 2 and 3) correspond to photon polarization along the x axis (polarization in the production plane), while the perpendicular ones (columns 4 and 5) correspond to polarization normal to the production plane (along the y axis). The subscripts represent, respectively, the initial and final proton polarization states, always quantized with respect to the incident photon direction (z axis).

The conditions represented in Table II (photoproduction at 90° in the center-of-mass system by plane-polarized photons) are precisely those studied in the experiments of Alspector *et al.*¹⁴ In this paper, we compare these observations for the two reactions

$$\gamma + p \rightarrow n + \pi^+ \quad (1a)$$

and

$$\gamma + p \rightarrow p + \pi^0 \quad (1b)$$

for photon energies between 0.8 and 1.6 GeV.¹⁵

For comparison with these experiments, we have explored the predictions of the quark model

TABLE II. Relevant amplitudes for electric and magnetic photoexcitation of intermediate resonances, relative to the conventional helicity frame (all proton helicities measured with respect to z axis, scattering in x - z plane).

Intermediate resonance, J^P	$A_{1/2 \rightarrow 1/2}^{\parallel}$	$A_{1/2 \rightarrow -1/2}^{\parallel}$	$A_{1/2 \rightarrow 1/2}^{\perp}$	$A_{1/2 \rightarrow -1/2}^{\perp}$
$\frac{1}{2}^+$	\mathcal{G}_{M1}	0	$-i\mathcal{G}_{M1}$	0
$\frac{1}{2}^-$	0	$-\mathcal{G}_{E1}$	0	$i\mathcal{G}_{E1}$
$\frac{3}{2}^+$	$-(\mathcal{G}_{M1} + \sqrt{3}\mathcal{G}_{E2})$	0	$-2i\mathcal{G}_{M1}$	0
$\frac{3}{2}^-$	0	$-2\mathcal{G}_{E1}$	0	$-i(\sqrt{3}\mathcal{G}_{M2} + \mathcal{G}_{E1})$
$\frac{5}{2}^+$	$-\frac{1}{2}(\frac{3}{2})^{1/2}\mathcal{G}_{M3} + \sqrt{3}\mathcal{G}_{E2}$	0	$i\frac{3}{2}(\frac{3}{2})^{1/2}\mathcal{G}_{M3}$	0
$\frac{5}{2}^-$	0	$\frac{3}{2}(\frac{3}{2})^{1/2}\mathcal{G}_{E3}$	0	$i[\sqrt{3}\mathcal{G}_{M2} - \frac{1}{2}(\frac{3}{2})^{1/2}\mathcal{G}_{E3}]$

described above, very much along the same lines as in the aforementioned work of Faiman and Hendry,⁶ of Copley, Karl, and Obryk,⁷ and of Walker.¹²

II. THE QUARK MODEL

The spectrum of baryonic states of zerostrangeness (hypercharge-1), according to the latest particle data compilation,¹⁶ is shown in Fig. 1. It may be noted that the levels tend to cluster into bands of alternating parity, which may be associated with the level ordering predicted by the (qqq) harmonic-oscillator model. This level scheme, together with the quantum numbers associated with the first three groups of levels (supermultiplets), is summarized in Table III.

Thus, assuming wave functions symmetric with respect to quark interchange, the ground level ($E_1 = \frac{3}{2}\hbar\omega$) would be an SU(6) 56-plet with total internal angular momentum $L=0$ and positive parity, containing the nucleons [SU(3) octet with spin $\frac{1}{2}$, or P_{11}] and the $\Delta(1236)$ resonance with spin and isospin $\frac{3}{2}$ [SU(3) decimlet with spin $\frac{3}{2}$, or P_{33}]. The next level ($E_2 = \frac{5}{2}\hbar\omega$) is expected to be an SU(6) 70-plet, with $L=1$, negative parity and mixed spatial symmetry, whose SU(3) \times SU(2) decomposition is shown in Table III. Note that all the baryonic members of this supermultiplet have been identified (i.e., refer to cluster 2 in Fig. 1, and to Table IV).

However, the situation degenerates rapidly as one proceeds to higher supermultiplets, owing to the rapid accumulation of available states. Thus the $n=3$ level ($E_3 = \frac{7}{2}\hbar\omega$) contains the possibility of 13 nucleonlike and 8 Δ -like states, all presumably associated with cluster 3 in Fig. 1. It is interest-

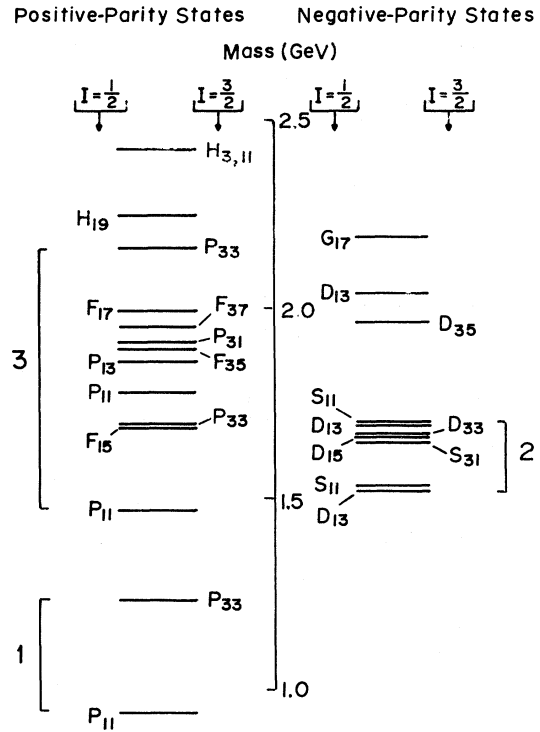


FIG. 1. Spectrum of observed $N^*(I = \frac{1}{2})$ and $\Delta^*(I = \frac{3}{2})$ resonances.

ing that, with just two exceptions,¹⁷ these could all be associated with the $(56, 0^+)$ and $(56, 2^+)$ members of the $n=3$ supermultiplet, as might be expected if the internal (degeneracy-removing) forces among quarks strongly favored spatially symmetric states

TABLE III. Predicted quark-model spectrum of nonstrange baryons.

Energy level	SU(6) assignment (multiplet, L^P)	Octets ($I = \frac{1}{2}$) multiplet (S), ($l_{\pi 2I, 2J}$)	Decimets ($I = \frac{3}{2}$) multiplet (S), ($l_{\pi 2I, 2J}$)
1	$(56, 0^+)$	$8(\frac{1}{2}), (P_{11})$	$10(\frac{3}{2}), (P_{33})$
2	$(70, 1^-)$	$8(\frac{3}{2}), (D_{15}, D_{13}, S_{11})$	$10(\frac{1}{2}), (D_{33}, S_{31})$
		$8(\frac{1}{2}), (D_{13}, S_{11})$	
3	$(56, 0^+)$	$8(\frac{1}{2}), (P_{11})$	$10(\frac{3}{2}), (P_{33})$
	$(70, 0^+)$	$8(\frac{3}{2}), (P_{13})$	
		$8(\frac{1}{2}), (P_{11})$	$10(\frac{1}{2}), (P_{31})$
	$(56, 2^+)$	$8(\frac{1}{2}), (F_{15}, P_{13})$	$10(\frac{3}{2}), (F_{37}, F_{35}, P_{33}, P_{31})$
	$(70, 2^+)$	$8(\frac{3}{2}), (F_{17}, F_{15}, P_{13}, P_{11})$	
		$8(\frac{1}{2}), (F_{15}, P_{13})$	$10(\frac{1}{2}), (F_{35}, P_{33})$
	$(20, 1^+)$	$8(\frac{1}{2}), (P_{13}, P_{11})$	

(see Table IV).

In this way, we have attempted in Table IV to associate observed states with the members of the basic (56, L -even) and (70⁻, L -odd) multiplets and their recurrences. It is, of course, important to note that in the case of such a multiplet structure, the degeneracy-removing forces will also tend to mix states with the same values of I , J , and parity. We shall have more to say about the mixing problem later on.

Finally, we note from Fig. 1 that the spacing between the $n=1$ and $n=2$ clusters would correspond to a harmonic-oscillator frequency ($\hbar\omega$) of ≈ 500 MeV, although the spacing of the higher- n -value clusters seems to be somewhat less.¹⁸

The baryon, composed of three quarks, may be excited much like a triatomic molecule, into states of higher rotational angular momentum. Computation of matrix elements is straightforward if we assume that photon absorption by a single quark is the dominant mechanism of excitation in photo-production.^{6,7} In this model, the interaction of a quark with a photon depends on three parameters.

(1) The magneton of the quark, which is usually taken equal to the magnetic moment of the proton¹⁹

$$\mu_q = \mu_p = \left(\frac{g}{2}\right) \frac{e}{2M_q} = 2.79 \frac{e}{2M_p},$$

where μ_q =quark magneton, e =unit charge, M_q =effective quark mass, and g =the gyromagnetic ratio (2 for a Dirac moment). $g=2$ then implies $M_q=0.34$ GeV.

(2) The harmonic-oscillator parameter is given by $\alpha^2 = \omega M_q$. For $M_q=0.34$ GeV and $\omega = \frac{1}{2}$ GeV we obtain $\alpha^2 = 0.17$ (GeV)². This agrees with the choice of Copley *et al.*⁷ which leads to vanishing of the F_{15} amplitudes at 0° and 180°, as indicated by experiment.²⁰ However, an analysis of the experimental uncertainties implies that α^2 is only determined to within roughly a factor of 2 by this method. In this work we will allow α^2 to vary within these rough limits in order to obtain the best fit to the experimental data of Alspector *et al.*¹⁴

(3) The value of g has been chosen to be $g=2$. This would correspond to a structureless, Dirac quark. However, in the spirit of the quark model, this choice is an arbitrary one, just as long as we keep the ratio M_q/g constant at 0.17 GeV [condition (1) above]. Note that, by this criterion, a large g implies a large M_q , and vice versa. However, too large an increase in M_q would upset the value of the parameter α^2 which,²¹ as we shall see in the analysis that follows, should not exceed ≈ 0.2 GeV² by a very large factor. Thus, we are here again confronted with the classic quark-model dilemma of computations requiring quarks of such small mass that they should not have eluded observation

TABLE IV. Nonstrange baryon resonances^a from the Particle Data Group compilation (see Ref. 16) and possible quark-model assignments.

Oscillator level				
1	$P_{11}(939)$	(56, 0 ⁺ - 8 ₂)	$P_{33}(1232)$	(56, 0 ⁺ - 10 ₄)
2	$D_{13}(1520)$ } $S_{11}(1535)$ }	(70, 1 ⁻ - 8 ₂)	$S_{31}(1650)$ } $D_{33}(1670)$ }	(70, 1 ⁻ - 10 ₂)
	$D_{15}(1670)$ } $S_{11}(1700)$ } $[D_{13}(1700)]$ }	(70, 1 ⁻ - 8 ₄)		
3	$P_{11}(1470)$ } $F_{15}(1688)$ } $P_{13}(1810)$ }	(56, 0 ⁺ - 8 ₂) (56, 2 ⁺ - 8 ₂)	$[[P_{33}(1690)]]$ $F_{35}(1890)$ } $P_{31}(1910)$ } $F_{37}(1950)$ } $[[P_{33}(2160)]]$ }	(56, 0 ⁺ - 10 ₄) (56, 2 ⁺ - 10 ₄)
4	$[D_{13}(2040)]$ $[[S_{11}(2100)]]$ $[[D_{15}(2100)]]$ $G_{17}(2190)$	(70, 1 ⁻ + 3 ⁻ - 8 ₂ + 8 ₄) (70, 1 ⁻ - 8 ₂ + 8 ₄) (70, 1 ⁻ + 3 ⁻ - 8 ₂ + 8 ₄) (70, 3 ⁻ - 8 ₂ + 8 ₄)	$[[S_{31}(1900)]]$ $[D_{35}(1960)]$	(70, 1 ⁻ - 10 ₂) (70, 3 ⁻ - 10 ₂)
5	$P_{11}(1780)$ $[F_{17}(1990)]$ $[F_{15}(2000)]$ $H_{19}(2220)$	(56, 0 ⁺ - 8 ₂) (56, 4 ⁺ - 8 ₂) (56, 2 ⁺ - 8 ₂) (56, 4 ⁺ - 8 ₂)	$H_{3,11}(2420)$	(56, 4 ⁺ - 10 ₄)

^a The number of brackets surrounding the resonance indicates the degree of uncertainty of the identification.

if they were real. We adopt, here, the classic solution to this dilemma—which is to ignore it.

With the above choice of parameters we can now compute the amplitude for photoexcitation of any of the baryon resonances contained in Table III. In terms of the $A_{\pm 1/2}$ and $A_{\pm 3/2}$ amplitudes,²² as defined, e.g., by Copley *et al.*⁷ or in the Particle Data Group compilation,¹⁶ the cross sections for

pion photoproduction by photons polarized either parallel or perpendicular to the production plane are given by

$$\frac{d\sigma}{d\Omega}^{\parallel, \perp} = 2(|A_{nf}^{\parallel, \perp}|^2 + |A_f^{\parallel, \perp}|^2), \quad (2)$$

where, for $J_R = l_\pi + \frac{1}{2}$,

$$A_{nf}^{\parallel, \perp} = \text{nonflip amplitude} \\ = \left(\frac{1}{4\pi}\right)^{1/2} \sum_{\text{resonances}} \left[(C_{\pi N}^I)^2 \frac{\chi}{\Gamma} \frac{M_N}{M_R} \right]^{1/2} \left\{ - \left[\frac{(l+2)}{l(l+1)} \right]^{1/2} P_l^1 e^{i\varphi} A_{3/2} \pm \left[\frac{1}{(l+1)} \right]^{1/2} P_l^1 e^{-i\varphi} A_{-1/2} \right\}, \quad (3a)$$

$$A_f^{\parallel, \perp} = \text{flip amplitude} \\ = \left(\frac{1}{4\pi}\right)^{1/2} \sum_{\text{resonances}} \left[(C_{\pi N}^I)^2 \frac{\chi}{\Gamma} \frac{M_N}{M_R} \right]^{1/2} \left\{ \left[\frac{1}{l(l+1)(l+2)} \right]^{1/2} P_l^2 e^{2i\varphi} A_{3/2} \pm (l+1)^{1/2} P_l^0 A_{-1/2} \right\} \quad (3b)$$

and for $J_R = l_\pi - \frac{1}{2}$,

$$A_{nf}^{\parallel, \perp} = \left(\frac{1}{4\pi}\right)^{1/2} \sum_{\text{resonances}} \left[(C_{\pi N}^I)^2 \frac{\chi}{\Gamma} \frac{M_N}{M_R} \right]^{1/2} \left\{ \left[\frac{(l-1)}{l(l+1)} \right]^{1/2} P_l^1 e^{i\varphi} A_{3/2} \mp \left(\frac{1}{l}\right)^{1/2} P_l^1 e^{-i\varphi} A_{-1/2} \right\}, \quad (4a)$$

$$A_f^{\parallel, \perp} = \left(\frac{1}{4\pi}\right)^{1/2} \sum_{\text{resonances}} \left[(C_{\pi N}^I)^2 \frac{\chi}{\Gamma} \frac{M_N}{M_R} \right]^{1/2} \left\{ \left[\frac{1}{l(l-1)(l+1)} \right]^{1/2} P_l^2 e^{2i\varphi} A_{3/2} \pm \sqrt{l} P_l^0 A_{-1/2} \right\}. \quad (4b)$$

In Eqs. (3) and (4),

M_N = nucleon mass,

M_R = resonance mass,

χ = elasticity = Γ_π/Γ at resonance,

J_R = spin of the resonance,

l_π = l = orbital angular momentum of the pion-nucleon system,

Γ = width of the resonance,

$C_{\pi N}^I$ = the Clebsch-Gordan coefficient in isospin space for the matrix element $\langle N^* | N \pi \rangle$.

Note that $A_{\pm 3/2}$ and $A_{\pm 1/2}$ are proportional to the matrix elements for absorption of photons of helicity ± 1 into intermediate (resonance) states of respectively, $m_J = \pm \frac{3}{2}$ and $m_J = \pm \frac{1}{2}$. While $|A_\lambda| = |A_{-\lambda}|$, their relative sign is determined by the appropriate Clebsch-Gordan coefficient associated with the spin-orbit coupling ($\vec{J} = \vec{L} + \vec{S}$) for the resonance of interest.

The computations using the quark-model wave functions give the values of the amplitudes at resonance, A_λ ; for extrapolating to energies off resonance, Breit-Wigner amplitudes were assumed, of the form

$$A_\lambda(y) = \frac{y - iy}{y^2 + \gamma^2} (i\gamma A_\lambda), \quad (5)$$

where $\lambda = \Gamma/2$ and $y = E - M_R$. For those cases where the tables gave a range of values of Γ , the smallest values were used, in order to separate as much as possible the contributions of the individual resonances, our purpose being to study the qualitative predictions of the model rather than to attempt a detailed, quantitative fitting of the experiments.

In Table V we list the matrix elements (A 's) for photoproduction of the resonances of interest. In listing the resonances we also show in parentheses the values of M_R , Γ (in MeV), and χ assumed. We note, first, the difference in dependence on the photon momentum, k , of the terms corresponding to the "orbital" and the "spin" contributions, $R_{i,1}$ and $R_{i,0}$, respectively; the coefficients of the latter are proportional to $k^{1/2}$ while the former decrease with increasing momentum like $k^{-1/2}$. Then, the dependence of the various "form factors" R_{ij} on (k/α) is of interest. Aside from the expected Gaussian $e^{-k^2/6\alpha^2}$, the coefficients reflect the wavelength dependence of the different electric and magnetic multiplicities associated with the various transitions in question. (See Table II for a comparison with the conventional multipole description.)

III. THE FITTING PROCEDURE

The data we have tried to fit are shown in Fig. 2. In this figure we have drawn freehand curves cor-

responding to the limits of the uncertainties as shown. Since our analysis only included excited states of energy $M_R \lesssim 2$ GeV, we shall only carry our comparison with the experimental data up to the corresponding $E_\gamma \lesssim 1.6$ GeV.

We began by fitting the data for $\gamma + p \rightarrow n + \pi^+$; we first tried the Copley⁷ value for α ($\alpha = 0.41$). The results are shown in Fig. 3. The predicted curves are indicated by crosses (X). We note that the computed points generally tend to fall below the experimental values for γ_{\parallel} , but not for γ_{\perp} . One way of raising the predicted values is through the form factor's dependence on the oscillator parameter, α . Thus, we tried to see the effect of increasing α , thereby increasing the value of the exponential form factor and hence raising the predicted cross sections. The results for $\alpha = 0.71$,

shown in Fig. 3 by circles (O), clearly overshoot the intended effect in the case of γ_{\perp} , although the predicted curve for γ_{\parallel} is reasonable in this case. Hence we settled on $\alpha = 0.51$ as a reasonable compromise to the value giving the best fit. The results are shown in Fig. 4 for reactions (1a) and in Fig. 5 for reactions (1b).

The most interesting point to note, in considering Figs. 4 and 5, is that our model reproduces the most significant qualitative features of the energy dependence of the observed cross sections, although the detailed fits leave much to be desired. It is interesting, with respect to the π^+ production, that the predicted points for the two directions of photon polarization are either all too low [Fig. 4(a)] or too high [Fig. 4(b)]. This is somewhat suggestive of the possibility that the neglected background

TABLE V. Amplitudes for photoexcitation of baryon resonances for a proton target (after Copley *et al.*) $\bar{g} = g/2 = 1$ (Dirac moment).

Resonance (mass, width, elasticity)	$A_{1/2}$	$A_{3/2}$	SU(6) \times O(3) assignment
$P_{11}(1470, 165, 0.60)$	$2\sqrt{\pi k} \mu R_{00}^{S*}$...	$(56, 0^+), 8(\frac{1}{2}) (n=3)$
$D_{13}(1520, 105, 0.50)$	$(\frac{2}{3})^{1/2} \left(\frac{\pi}{k}\right)^{1/2} \frac{\mu}{g} (\sqrt{2} k \bar{g} R_{10}^\lambda - R_{11}^\lambda)$	$-\sqrt{2} \frac{\mu}{g} \left(\frac{\pi}{k}\right)^{1/2} R_{11}^\lambda$	$(70, 1^-), 8(\frac{1}{2}) (n=2)$
$S_{11}(1535, 50, 0.35)$	$\frac{-2}{\sqrt{3}} \left(\frac{\pi}{k}\right)^{1/2} \frac{\mu}{g} \left(\frac{1}{\sqrt{2}} k \bar{g} R_{10}^\lambda + R_{11}^\lambda\right)$...	$(70, 1^-), 8(\frac{1}{2}) (n=2)$
$D_{15}(1670, 105, 0.40)$	0	0	$(70, 1^-), 8(\frac{3}{2}) (n=2)$
$F_{15}(1688, 105, 0.60)$	$\frac{2\sqrt{2}}{\sqrt{5}} \left(\frac{\pi}{k}\right)^{1/2} \frac{\mu}{g} [(\frac{2}{3})^{1/2} k \bar{g} R_{20}^S - R_{21}^S]$	$\frac{-4}{\sqrt{5}} \frac{\mu}{g} \left(\frac{\pi}{k}\right)^{1/2} R_{21}^S$	$(56, 2^+), 8(\frac{1}{2}) (n=3)$
$S_{11}(1700, 100, 0.65)$	0	...	$(70, 1^-), 8(\frac{3}{2}) (n=2)$
$P_{13}(1860, 180, 0.25)$	$\frac{-2\sqrt{3}}{\sqrt{5}} \left(\frac{\pi}{k}\right)^{1/2} \frac{\mu}{g} [(\frac{2}{3})^{1/2} k \bar{g} R_{20}^S + R_{21}^S]$	$\frac{2}{\sqrt{5}} \frac{\mu}{g} \left(\frac{\pi}{k}\right)^{1/2} R_{21}^S$	$(56, 2^+), 8(\frac{1}{2}) (n=3)$
$[D_{13}(1680, 128, 0.33)]$	0	0	$(70, 1^-), 8(\frac{3}{2}) (n=2)$
$P_{33}(1236, 110, 0.994)$	$\frac{-2\sqrt{2}}{3} \sqrt{\pi k} \mu R_{00}^S$	$-2(\frac{2}{3})^{1/2} \sqrt{\pi k} \mu R_{00}^S$	$(56, 0^+), 10(\frac{3}{2}) (n=1)$
$S_{31}(1650, 130, 0.28)$	$\frac{-2}{\sqrt{3}} \left(\frac{\pi}{k}\right)^{1/2} \frac{\mu}{g} \left(\frac{k \bar{g}}{3\sqrt{2}} R_{10}^\lambda - R_{11}^\lambda\right)$...	$(70, 1^-), 10(\frac{1}{2}) (n=2)$
$D_{33}(1670, 175, 0.15)$	$-\left(\frac{2}{3}\right)^{1/2} \left(\frac{\pi}{k}\right)^{1/2} \frac{\mu}{g} \left(\frac{\sqrt{2} k \bar{g}}{3} R_{10}^\lambda + R_{11}^\lambda\right)$	$-\sqrt{2} \left(\frac{\pi}{k}\right)^{1/2} \frac{\mu}{g} R_{11}^\lambda$	$(70, 1^-), 10(\frac{1}{2}) (n=2)$
$F_{35}(1890, 135, 0.17)$	$\frac{2\sqrt{2}}{\sqrt{105}} \sqrt{\pi k} \mu R_{20}^S$	$\frac{12}{\sqrt{105}} \mu \sqrt{\pi k} R_{20}^S$	$(56, 2^+), 10(\frac{3}{2}) (n=3)$
$P_{31}(1910, 230, 0.25)$	$\frac{2\sqrt{2}}{3\sqrt{5}} \sqrt{\pi k} \mu R_{20}^S$...	$(56, 2^+), 10(\frac{3}{2}) (n=3)$
$F_{37}(1950, 140, 0.45)$	$\frac{-4}{\sqrt{35}} \sqrt{\pi k} \mu R_{20}^S$	$\frac{4}{\sqrt{21}} \sqrt{\pi k} \mu R_{20}^S$	$(56, 2^+), 10(\frac{3}{2}) (n=3)$

$$R_{00}^S = e^{-k^2/6\alpha^2}, \quad R_{00}^{S*} = -\frac{1}{2\sqrt{3}} \frac{k^2}{3\alpha^2} e^{-k^2/6\alpha^2}, \quad R_{10}^\lambda = \frac{ik}{\sqrt{3}\alpha} e^{-k^2/6\alpha^2},$$

$$R_{11}^\lambda = i\left(\frac{2}{3}\right)^{1/2} \alpha e^{-k^2/6\alpha^2}, \quad R_{20}^S = -\frac{1}{6} \left(\frac{2}{3}\right)^{1/2} \left(\frac{k}{\alpha}\right)^2 e^{-k^2/6\alpha^2}, \quad R_{21}^S = -\frac{1}{3} k e^{-k^2/6\alpha^2}.$$

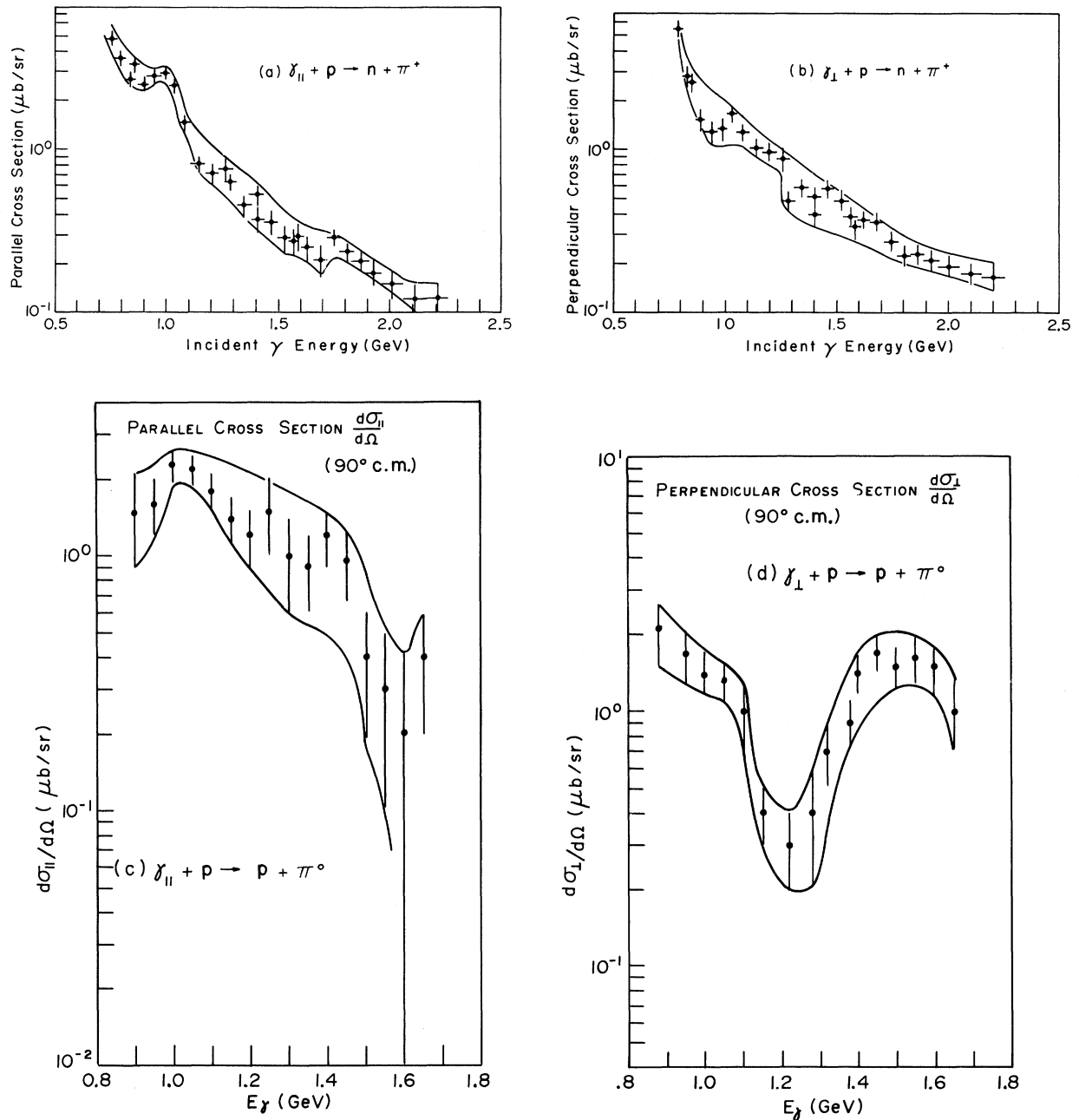


FIG. 2. Data of Alspector *et al.* (see Ref. 14) on photomeson production at 90° in the c.m. system by polarized photons.

effects may tend to interfere in opposite directions in the two cases. For both polarizations, however, the qualitative fit is worst at the lowest energies (a point to which we shall return).

For the π^0 production, on the other hand, the fits tend to be reasonable at the low-energy end, while lying consistently on the low side for the higher energies. Generally speaking, we should

not be too greatly surprised or concerned over this kind of behavior, since we have neglected resonances of energy above $E_{\gamma} \cong 1.6$ GeV ($M_R \cong 2$ GeV) in our analysis.

Returning to the problem of the low-energy behavior exhibited in Fig. 4, one may note that the most important contribution to our predicted cross section in the energy range 0.8–1.2 GeV comes

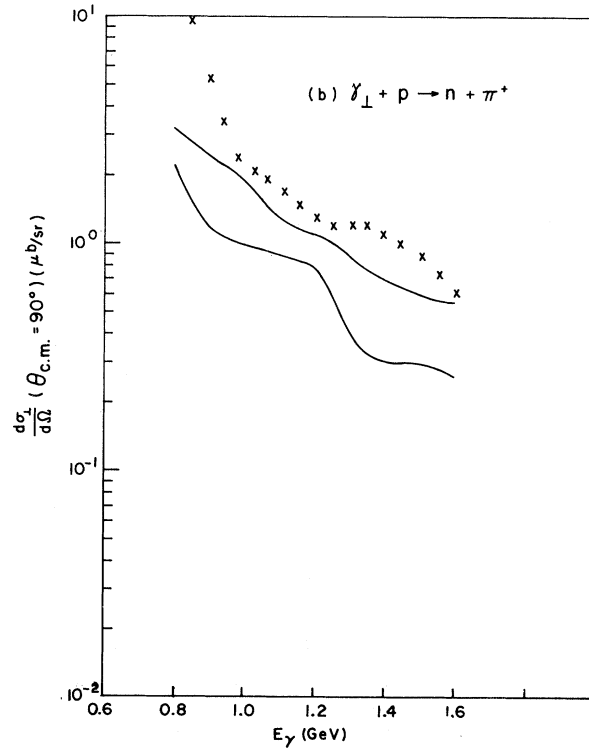
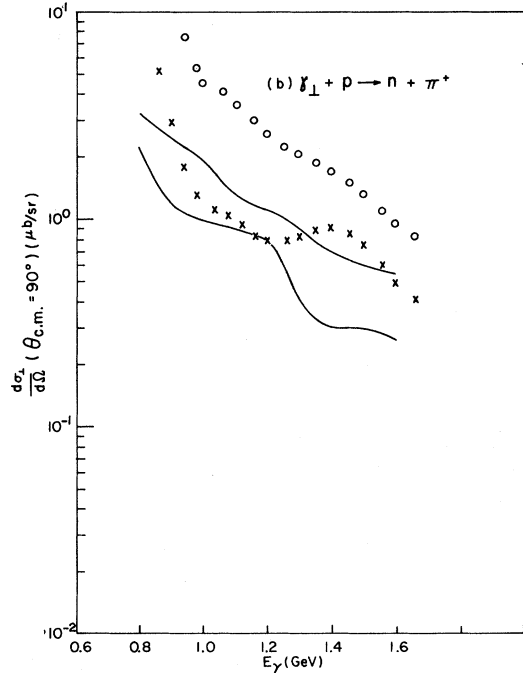
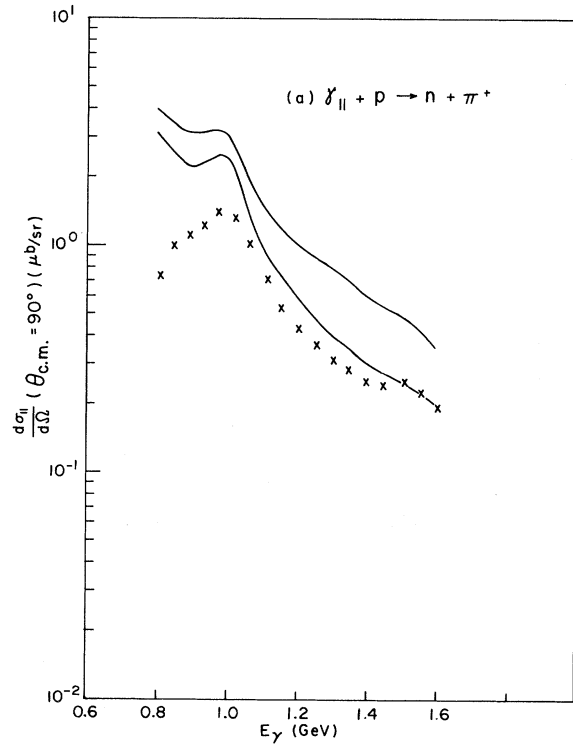
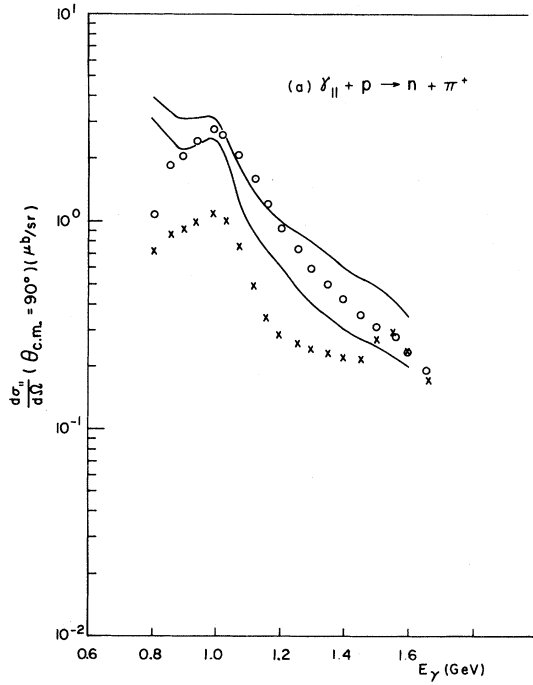


FIG. 3. Comparison of experiment with the predictions of the quark model for two values of the oscillator parameter α , 0.41 (x) and 0.71 (o). (a) $\gamma_{\parallel} + p \rightarrow n + \pi^+$, (b) $\gamma_{\perp} + p \rightarrow n + \pi^+$. The crosses and circles refer, respectively, to the assumption $\alpha = 0.41$ and 0.71 for the value of the harmonic-oscillator parameter.

FIG. 4. Comparison of experiment with the predictions of the quark model for $\alpha = 0.51$ GeV. (a) $\gamma_{\parallel} + p \rightarrow n + \pi^+$, (b) $\gamma_{\perp} + p \rightarrow n + \pi^+$.

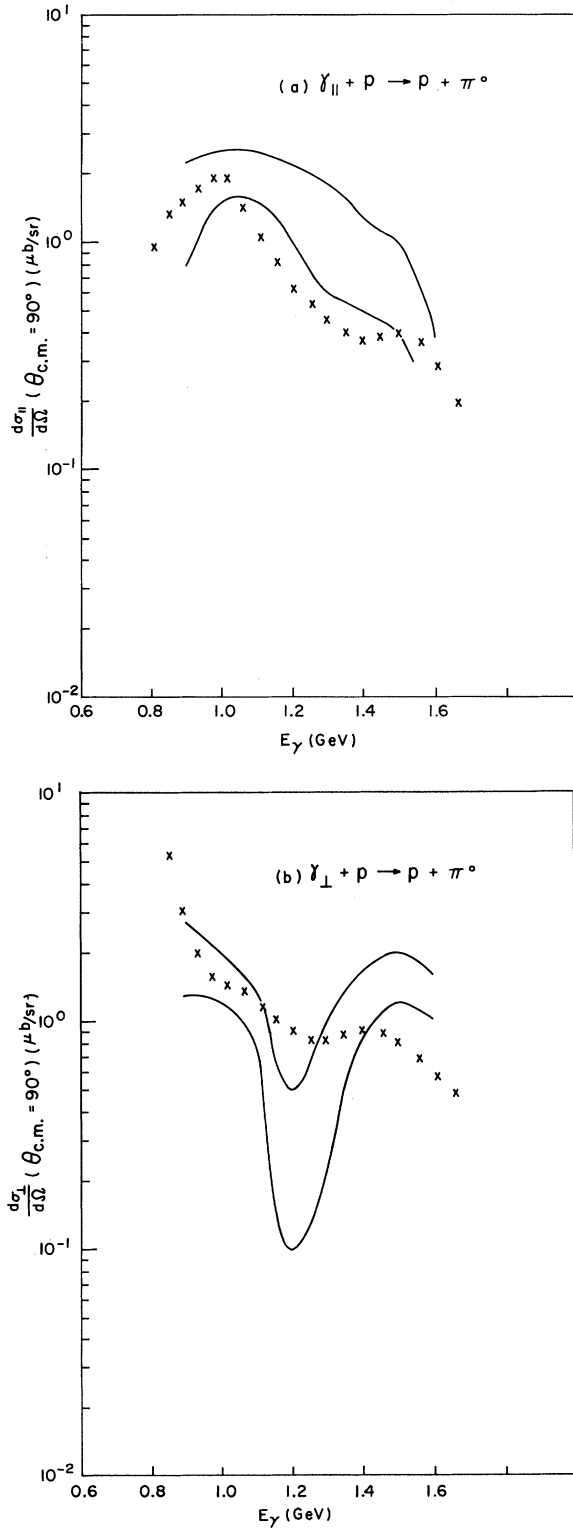


FIG. 5. Comparison of experiment with the predictions of the quark model for $\alpha = 0.51$ GeV. (a) $\gamma_{\parallel} + p \rightarrow p + \pi^0$, (b) $\gamma_{\perp} + p \rightarrow p + \pi^0$.

from the $S_{11}(1535)$ resonance. We find that the (arbitrary) elimination of this resonance results in a much improved fit (Fig. 6).

IV. EFFECTS OF RESONANCE MIXING

This last observation is suggestive of an effect which we have thus far neglected—that of the mixing of resonances of the same spin and parity. Within the $n=2$ ($70, 1^-$) supermultiplet, there are two such states, the S_{11} and the D_{13} (see Table III), each of which appears both in the spin quartet and in the spin doublet SU(3) octets.²³ Symmetry-breaking forces such as those responsible for the energy splitting will generally also give rise to resonance-mixing effects.

Such effects have previously been considered by Faiman and Hendry⁶ in their analysis of resonance decay widths and branching ratios. Using the conventional definitions of the resonance mixing angles θ_1 and θ_3

$$S_{11}(1535) = \cos \theta_1 S_{11}(8_2) - \sin \theta_1 S_{11}(8_4), \quad (6a)$$

$$S_{11}(1700) = \sin \theta_1 S_{11}(8_2) + \cos \theta_1 S_{11}(8_4) \quad (6b)$$

[and analogously for θ_3 for $D_{13}(1520)$ and $D_{13}(1700)$ mixing], we have explored the effects of different assumptions for the values of θ_1 and θ_3 . In particular, since we were faced with a double-infinity of possible mixing angle combinations, we have been guided by the values suggested by Faiman and Hendry,

$$\theta_1 \approx 35^\circ \text{ or } 90^\circ, \quad (7a)$$

$$\theta_3 \approx 35^\circ \text{ or } 127^\circ. \quad (7b)$$

However, we have also tried a number of other combinations.

The results of this exploration have been rather surprising (and disappointing); we have not been able to improve substantially the fits shown in Figs. 4, 5, or 6 by any of the θ_1 - θ_3 combinations we have tried.

Two examples of such attempts are shown in Fig. 7. Thus, in Figure 7(a) we show the predictions for the reaction $\gamma_{\parallel} + p \rightarrow n + \pi^+$ [compare with Fig. 4(a)] for the values $\theta_1 = 90^\circ$, $\theta_3 = 35^\circ$ (\circ), and $\theta_1 = 90^\circ$, $\theta_3 = 130^\circ$ (\times). Note that while the fit at the lower energies is substantially improved, especially in the 90° - 35° combination, the effect of moving the $S_{11}(8_2)$ resonance from 1535 to 1700 MeV is to effectively destroy the fit at the higher energies.

A similar phenomenon is noted in Figure 7(b), in which the predictions for $\gamma_{\perp} + p \rightarrow n + \pi^+$ are shown for the combination $\theta_1 = 35^\circ$, $\theta_3 = 35^\circ$ (\circ) and 35° - 130° (\times) [compare with Fig. 4(b)]. All of our other attempts to improve the fits via a variety

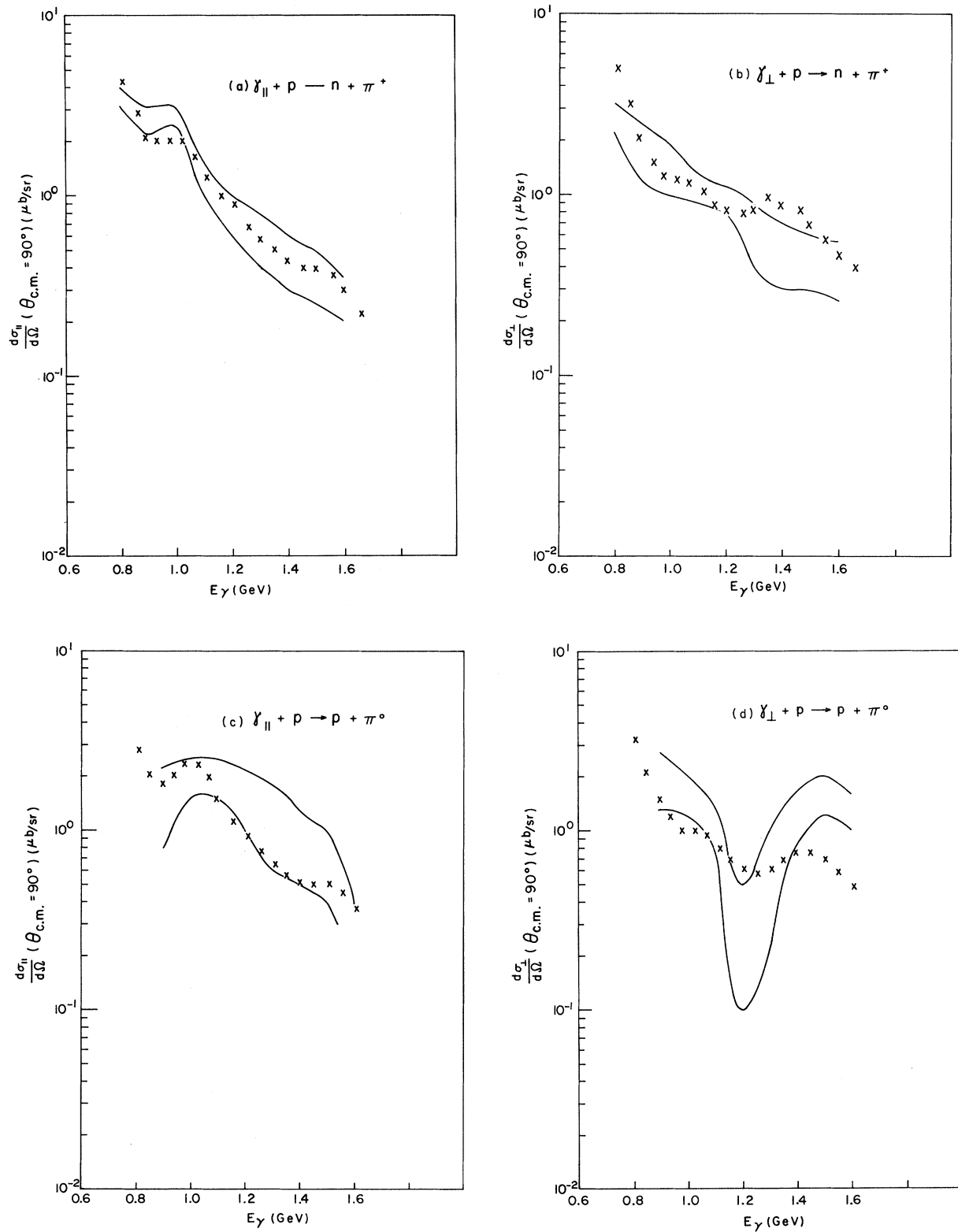


FIG. 6. Comparison of experiment with the predictions of the quark model for $\alpha=0.51$, with the $S_{11}(1535)$ resonance omitted. (a) $\gamma_{||} + p \rightarrow n + \pi^+$, (b) $\gamma_{\perp} + p \rightarrow n + \pi^+$, (c) $\gamma_{||} + p \rightarrow p + \pi^0$, and (d) $\gamma_{\perp} + p \rightarrow p + \pi^0$.

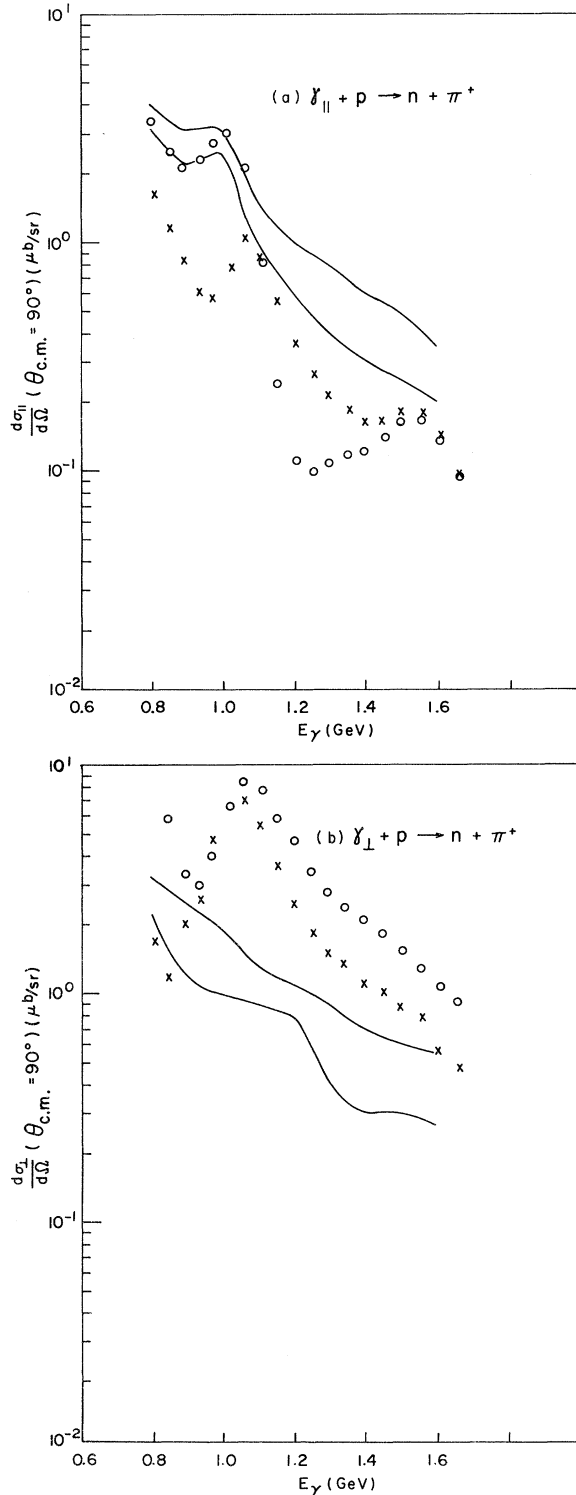


FIG. 7. (a) $\gamma_{\parallel} + p \rightarrow n + \pi^+$ predictions for two mixing angle combinations (see text). (b) $\gamma_{\perp} + p \rightarrow n + \pi^+$ predictions for two (other) mixing angle combinations. The circles refer to the assumption $\theta_1 = 90^\circ$, $\theta_3 = 35^\circ$ while the crosses assume $\theta_1 = 90^\circ$, $\theta_3 = 130^\circ$ for the mixing angles of the two $s_{11}(\theta_1)$ and $D_{13}(\theta_3)$ resonances, respectively.

of θ_1 - θ_3 combinations have been equally disappointing.

V. SUMMARY AND CONCLUSIONS

Taking into account the known baryon resonances up to $M_R \approx 2$ GeV, we were able to obtain reasonable qualitative fits to the data of Alspector *et al.*¹⁴ for single-pion photoproduction in the resonance region by plane polarized photons, polarized both in the production plane (parallel) and normal to the production plane (perpendicular). Breit-Wigner forms were taken for the resonance amplitudes. The strengths of the perpendicular and parallel photoproduction amplitudes were derived on the basis of an $SU(6) \times O(3)$ conventional quark model, in which the baryon states are assumed to be appropriate three-quark combinations. The even-parity resonances were assigned to the 56-plet $SU(6)$ representation, and odd-parity states to the 70^- representation. Background effects, such as t -channel exchanges or the Born term, were not included in the computations. Furthermore we included resonances only up to mass 2 GeV. Nevertheless, we obtained good qualitative fits to the data for the perpendicular and parallel cross sections corresponding to the reactions $\gamma + p \rightarrow n + \pi^+$ and $\gamma + p \rightarrow p + \pi^0$. We found that the over-all fits were improved if, instead of choosing for the harmonic-oscillator well-width parameter $\alpha = 0.41$, as suggested in the paper of Copley *et al.*,⁷ we choose $\alpha = 0.51$, a slightly higher value corresponding to a smaller baryon size. This value of α still leaves appreciable discrepancies in the quantitative aspects of the fits, although the shapes of the predicted curves of cross section vs energy are in generally good agreement with the experiments. However, we believe that the remaining discrepancies may be accounted for in terms of neglected background effects and of higher resonances—not included in our analysis—as well as of level mixing.

The main problems with our model—both conceptually and in its actual application—are associated with the problem of level mixing or, in any case, of the conventional assignment of the $S_{11}(1535)$ and $D_{13}(1520)$ to the quark spin doublet octet of $SU(2) \times SU(3)$; their spin-quartet twins are then associated with the low-angular momentum, negative-parity levels indicated by the conventional phase-shift analyses^{12,16} in the region $M_R \approx 1700$ MeV. Assuming the general, qualitative validity of our analysis, the indications are that there is considerable admixture of spin-quartet in the lower-lying levels, but that the spin-doublet levels are not appreciably present in the 1700 MeV ener-

gy region. This is, of course, contrary to the normal operation of simple level mixing.

However, it should also be noted¹⁶ that there may be a third S_{11} - D_{13} doublet in the mass region 2000-2100 MeV (see Table IV) presumably belonging to the $n=4$, 70^- SU(6) supermultiplet. These are sufficiently close in energy so that their mixing with the other two doublets should not be neglected. This renders the mixing problem sufficiently complex, and its possible solutions sufficiently ambiguous, so that we cannot exclude a situation in which the two lower energy pairs are very appreciably quark-spin $\frac{3}{2}$.

In this connection, in a comparison by Copley *et al.*⁷ of observed backward pion photoproduction in the resonance region with the predictions based on the parameters from Walker's analysis,¹² it was also found that the same $S_{11}(1535)$, assumed to be the 8_2 member, gave rise to difficulties. These difficulties, as in our case, could be overcome by an arbitrary reduction of the predicted strength of this level.

Generally the $D_{13}(8_2)$ resonance is less important in photoproduction from protons, and hence the analysis is rather less sensitive to its mixing properties. In any case, as is indicated in Fig. 7, the assumption of appreciable mixing between the 1520 MeV and an assumed 1700-MeV level does not improve the agreement between predictions and observations.

In conclusion, we again call attention to the qualitative success of the harmonic-oscillator quark model, as applied in this paper and others, in reproducing the observations in pion photoproduction by polarized as well as unpolarized photons. There remain some unresolved ambiguities; but insofar as the model requires relatively large symmetry-breaking forces, with the attendant mixing of levels within and between supermultiplets, such ambiguities may well be inherent in the model. In any case, it would appear to be useful to consider this problem further, as well as to improve these computations by the inclusion of background effects neglected by us.

*Work supported in part through funds provided by ERDA under No. Contract AT(11-1)-3069.

†Fulbright Research Scholar, 1974/75.

¹R. van Royen and V. F. Weisskopf, *Nuovo Cimento* **50**, 617 (1967); S. B. Berger and B. T. Feld, *Phys. Rev. D* **8**, 3875 (1973).

²B. T. Feld, *Models of Elementary Particles* (Ginn-Blaisdell, Boston, 1969); J. Kokkedee, *The Quark Model* (Benjamin, New York, 1969); A. J. G. Hey, P. J. Litchfield, and R. J. Cashmore, in *Proceedings of the XVII International Conference on High Energy Physics, London, 1974*, edited by J. R. Smith (Rutherford Laboratory, Chilton, Didcot, Berkshire, England, 1974), p. II-120; T. Abdullah and F. E. Close, *Phys. Rev. D* **5**, 2332 (1972).

³M. Gell-Mann, *Phys. Lett.* **8**, 214 (1964); G. Zweig, CERN Report No. TH 492, 1964 (unpublished).

⁴The antiquarks ($\bar{q} = \bar{u}, \bar{d}, \bar{s}$) have $B = -\frac{1}{3}$, spin and isospin unchanged, and the rest of the quantum numbers of opposite sign as compared to the corresponding quarks, q , in Table I.

⁵R. H. Dalitz in *High Energy Physics, École d'Été de Physique Théorique, Les Houches* (Gordon and Breach, New York, 1965).

⁶D. Faiman and A. W. Hendry, *Phys. Rev.* **173**, 1720 (1968); **180**, 1572 (1969). See also J. Babcock and J. L. Rosner, Report No. CALT-68-485, 1975 (unpublished); W. Petersen, *Phys. Rev. D* **12**, 2700 (1975).

⁷L. A. Copley, G. Karl, and E. Obryk, *Nucl. Phys.* **B13**, 303 (1969).

⁸H. Feshbach and L. S. Kisslinger, *Ann. Phys. (N.Y.)* **66**, 651 (1971).

⁹R. P. Feynman, M. Kislinger, and F. Ravndal, *Phys. Rev. D* **11**, 2706 (1971).

¹⁰S. D. Drell and K. Johnson, *Phys. Rev. D* **6**, 3248 (1972).

¹¹R. P. Feynman, *Photon-Hadron Interactions* (Benjamin, Reading, Mass., 1972).

¹²R. L. Walker, *Phys. Rev.* **182**, 1729 (1969).

¹³These remarks are obviously qualitative in nature, based on our experience with semiclassical phenomena in a generally nonrelativistic energy range. It is quite remarkable, however, how far such simple, qualitative predictions are borne out in the detailed calculations appropriate to the problem under consideration.

¹⁴J. Alspector *et al.*, *Phys. Rev. Lett.* **28**, 1403 (1972); J. Alspector, Ph.D. thesis, M.I.T., 1971 (unpublished); D. Fox, Ph.D. thesis, M.I.T., 1971 (unpublished); C. Nelson, Ph.D. thesis, M.I.T., 1971 (unpublished).

¹⁵The experiments actually employed photons up to 2.2 GeV in energy. However, since the nucleon excitation spectrum is not well established for isobar masses above ~ 2 GeV ($E_\gamma \sim 1.6$ GeV), we did not try to extend our analysis beyond this energy.

¹⁶Particle Data Group, *Phys. Lett.* **50B**, 1 (1974).

¹⁷These two exceptions are one superfluous P_{11} level and the F_{17} (1990) level. However, these might be associated with the next positive-parity ($n=5$) supermultiplet, together with the H_{19} and $H_{3,11}$ levels shown in Fig. 1; all of these, and many more, could then be considered as members of an $n=5$, $(56, 0^+) + (56, 2^+) + (56, 4^+)$ cluster with $E_5 = 11/2u$. Correspondingly, the cluster of negative-parity levels around 2 GeV can be associated with an $n=4$, $(70, 3^-)$ multiplet. See, also, P. J. Litchfield, in *Proceedings of the XVII International Conference on High Energy Physics, London, 1974*, edited by J. R. Smith (Rutherford Lab-

oratory, Chilton, Didcot, Berkshire, England, 1974), p. II-65; D. H. Lyth, in *ibid.*, p. II-147.

¹⁸By as much, perhaps, as a factor of 2.

¹⁹In the remainder of this paper, we adopt the system of units conventional to particle physics, with $\hbar = c = 1$, $e^2 = \frac{1}{137}$. Note that we have used the conventional definition of the g factor, which differs by a factor of 2 from that used by Faiman and Hendry (see Ref. 6).

²⁰R. L. Walker, Phys. Rev. 182, 1729 (1969).

²¹We can, but only to a limited extent, compensate for an increase in M_g by decreasing ω , but the observed level spectrum sets limits on ω .

²²The subscripts refer to the m_j value of the state resulting from one photon capture. Thus, $A_{1/2}$ and $A_{3/2}$ refer, respectively, to the amplitudes for the capture of right-circularly polarized photons ($m=1$) by protons

of polarization $m = -\frac{1}{2}$ and $m = \frac{1}{2}$, respectively.

²³Considering the possibility of mixing between different supermultiplets (different n values), there are many more candidates for mixing. Thus, P_{11} appears in the $(56, 0^+)$ groups for both $n=1$ and $n=3$, and P_{33} in $n=1$ $(56, 0^+)$, $n=3$ $(56, 0^+)$, and $n=3$ $(56, 2^+)$, etc. For odd-parity levels, even assuming only members of the $n=4$ 70^- representation of SU(6), there would be a possibility of mixing with two more S_{11} states, three more D_{13} , and three D_{15} . Of course, on our model, such mixing among supermultiplets would be diminished by the lack of overlap (or orthogonality) of radial wave functions, but there might still be non-negligible effects. However, we have neglected possible mixing between different supermultiplets in our analysis.